

Theory of Core-Level Photoemission and the X-ray Edge Singularity Across the Mott Transition

P. S. Cornaglia and A. Georges
*Centre de Physique Théorique, École Polytechnique,
CNRS-UMR 7644, 91128 Palaiseau Cedex, France.*
(Dated: February 6, 2008)

The zero temperature core-level photoemission spectrum of a Hubbard system is studied across the metal to Mott insulator transition using dynamical mean-field theory and Wilson's numerical renormalization group. An asymmetric power-law divergence is obtained in the metallic phase with an exponent $\alpha(U, Q) - 1$ which depends on the strength of both the Hubbard interaction U and the core-hole potential Q . For $Q \lesssim U_c/2$, α decreases with increasing U and vanishes at the transition ($U \rightarrow U_c$) leading to a symmetric peak in the insulating phase. For $Q \gtrsim U_c/2$, α remains finite close to the transition, but the integrated intensity of the power-law vanishes and there is no associated peak in the insulator. The weight and position of the remaining peaks in the spectra can be understood within a molecular orbital approach.

PACS numbers: 71.10.Fd, 71.30.+h, 79.60.-i

I. INTRODUCTION

When an incident x-ray photon ejects an electron from a core-level in a metal, the conduction band electrons feel a local attractive potential due to the created hole. It was discovered by Anderson¹ that the electronic ground states before and after the creation of the hole are orthogonal to each other. This many-body effect has dramatic consequences in x-ray photoemission spectroscopy (XPS) experiments where an asymmetric power-law divergence is observed.^{2,3,4} For a non-interacting metal, the exponent of the power-law and the relative intensity of the peaks in the XPS spectra are well understood. However, the behavior of the power-law divergence in a strongly interacting metal has received little theoretical attention besides the one-dimensional case.^{5,6}

Recently, there have been several XPS studies of strongly correlated transition-metal oxides,^{7,8,9,10} which addressed the changes in the core-level spectrum across the metal to Mott insulator transition (MIT). It was observed in particular that the (strongly renormalized) low-energy quasiparticles present in the metallic phase close to the MIT strongly modify the satellite peaks measured in XPS, an effect also discussed theoretically by Kim *et al.*⁸ In this paper, we provide a detailed theory of the core-level photoemission lineshape across the metal-insulator transition. A power-law behavior is found throughout the metallic phase up to the MIT where it is destroyed. Both the exponent and the intensity of the power-law are strongly renormalized by interactions and two different regimes can be identified depending on the ratio between the valence band interaction and the core-hole potential intensities.

The rest of the paper is organized as follows. In Sec. II we describe the model that we use in our calculations. The numerical results for the XPS spectra across the MIT transition are presented and discussed in Sec. III. Section IV contains the results of a molecular orbital approximation. Finally, we state the conclusions of our study

in Sec. V.

II. THE MODEL

The simplest model to study the correlation induced MIT is the Hubbard model

$$H = -t \sum_{\langle i,j \rangle \sigma} (c_{i\sigma}^\dagger c_{j\sigma} + c_{j\sigma}^\dagger c_{i\sigma}) + U \sum_i n_{i\uparrow} n_{i\downarrow} + \epsilon_d \sum_{i\sigma} n_{i\sigma},$$

where $c_{i\sigma}^\dagger$ creates an electron with spin σ at site i and $n_{i\sigma} = c_{i\sigma}^\dagger c_{i\sigma}$. A key quantity for this problem is the spectral function $A(\omega) = -\frac{1}{\pi} \text{Im}[G_{ii}(\omega + i0)]$ that contains information about the valence-band single particle photoemission spectrum. It can be obtained in the limit of large lattice coordination using dynamical mean-field theory (DMFT).¹¹ In the DMFT framework the Hubbard model reduces to an Anderson impurity model coupled to a non-interacting electron bath that is calculated in a self-consistent way.

In the XPS experiment a photon excites a core electron out of the sample and the resulting core-hole interacts with the band electrons attractively. In the sudden approximation considered below, the self-consistent bath remains unchanged while the energy of the effective Anderson impurity is shifted. The core-hole potential is taken as local and momentum independent^{2,3}

$$H_c = (\epsilon_h - Q \sum_\sigma c_{0\sigma}^\dagger c_{0\sigma}) h^\dagger h, \quad (1)$$

where $h^\dagger(h)$ creates (destroys) a core-hole at site 0, and ϵ_h is the core-level energy. In the sudden approximation the XPS spectrum is given by the core-hole spectral density

$$A_h(\omega) = \sum_{\nu_f} \delta(\omega - E_0^i + E_\nu^f + \epsilon_h) |\langle \nu_f | 0_i \rangle|^2, \quad (2)$$

where the final states $\{|\nu_f\rangle\}$ with corresponding energies $\{E_\nu^f\}$ satisfy the sum rule $\sum_{\nu_f} |\langle \nu_f | 0_i \rangle|^2 = 1$ and $|0_i\rangle$ is the initial ground state with energy E_0^i . The spectrum is zero for energies larger than the threshold energy $\omega_T \equiv E_0^i - E_0^f - \epsilon_h$ where E_0^f is the ground state energy in the final configuration.

In what follows we will consider a Bethe lattice geometry where the free density of states is given by¹¹

$$D(\omega) = \frac{2}{\pi D} \sqrt{1 - \left(\frac{\omega}{D}\right)^2}, \quad (3)$$

we will set the half-bandwidth $D \equiv 2t$ as the energy unit, and focus on half-filling ($\epsilon_d = -\mu = U/2$).

III. NUMERICAL RESULTS

In the non-interacting case ($U \rightarrow 0$) the spectral function $A(\omega)$ is simply given by Eq. (3) and the XPS spectrum then presents a Doniach-Šunjić power-law behavior at the threshold^{2,3,4,12,13}

$$A_h^0(\omega \rightarrow \omega_T) = \frac{\pi C_0}{\Gamma(\alpha) D} \left(\frac{\omega_T - \omega}{2D} \right)^{\alpha-1}, \quad \omega < \omega_T. \quad (4)$$

Here $C_0 \sim 1$, $\alpha = 2(\delta/\pi)^2 = 2/\pi^2 \arctan^2(2Q)$, where $\delta = \delta(\epsilon_F)$ is the phase-shift at the Fermi level due to scattering with the core-hole, and the factor 2 is due to spin degeneracy. For $Q > D/2$ a bound state appears in the final configuration that is reflected in the XPS spectra as an additional peak at $\omega - \omega_T \sim -Q$. These analytical results have been nicely reproduced numerically using Wilson's numerical renormalization group¹⁴ (NRG) by Líbero *et al.*¹³ Here we will use a different approach within the NRG scheme. To improve the accuracy at high energies we use a density matrix formulation.¹⁵ We have

$$A_h(\omega) = \sum_{\nu_f, \nu_i} \delta(\omega - E_\nu^i + E_\nu^f + \epsilon_h) \sum_{\nu'_i} \langle \nu_f | \nu_i \rangle \langle \nu_i | \rho | \nu'_i \rangle \langle \nu'_i | \nu_f \rangle,$$

where ρ is the density matrix. To evaluate the matrix elements $\langle \nu_f | \nu_i \rangle$ and $\langle \nu_i | \rho | \nu'_i \rangle$ two simultaneous runs of NRG are performed (with and without the core-hole energy shift). The $\langle \nu_f | \nu_i \rangle$ are calculated on the first iteration and then transformed to the new basis at each NRG iteration. The spectra are constructed following Ref. 16. The high numerical resolution of the NRG at low energies allows us to recover the power-law behavior with parameters that reproduce the analytical results (see Fig. 1). A bound state emerges in the final state for $Q > D/2$ and the associated peak in the XPS spectra can be observed at $\omega - \omega_T \sim -Q$.

For a non-zero Hubbard interaction, the spectral function $A(\omega)$ needs to be calculated in a self-consistent way. In what follows we will use the density matrix numerical renormalization group (NRG) scheme^{15,17,18} to solve

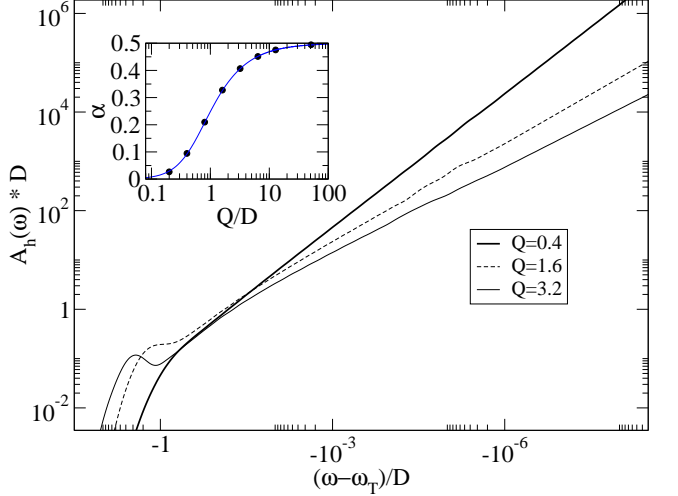


FIG. 1: (Color online) XPS spectra in the non-interacting case at electron-hole symmetry for different values of the core-hole potential Q . Inset: numerically obtained α (dots) and analytical expression $2/\pi^2 \arctan^2(2Q)$ (solid line).

the DMFT equations^{16,19} and to calculate the XPS spectra^{13,20} for different values of U . The ratio U/D can be varied in some materials across the MIT using chemical or mechanical pressure. The ratio U/Q , however, is expected to remain approximately constant for a given material. In Ref. 8 the spectra in Ru 3d systems were fitted using $Q = 1.25U$.

Figure 2a shows numerical results for the valence band spectral function. A small interaction in the band ($U \ll D$) produces only a slight modification of $A(\omega)$ that close to the Fermi level is approximately given by Eq. (3). For intermediate values of the interaction ($1.5 \lesssim U < U_c \simeq 2.95$) the system is in the strongly correlated regime and the valence band has a three peak structure. The central quasiparticle peak has a width $\sim zD$, where $z^{-1} = 1 - \partial \Re[\Sigma(\omega)] / \partial \omega|_{\omega=0}$ and $\Sigma(\omega)$ is the self-energy. The incoherent upper and lower Hubbard bands have a width $\sim D$ and their positions are determined by the atomic energies. The Fermi liquid behavior is restricted to a narrow region close to the Fermi level inside the quasiparticle peak which narrows with increasing interaction as $z \sim 0.3(U_c - U)$. For values of U larger than the critical interaction U_c the system is in the Mott insulator phase, there is no quasiparticle peak and the charge excitations are gapped.

Within the DMFT framework the interactions in the band produce a twofold modification of the non-interacting x-ray problem. The atomic level coupled to the core-hole potential has now a Hubbard interaction U and is hybridized with a renormalized electronic bath. To lowest order in U we may neglect the changes in the valence band and perform a Hartree-Fock approximation to treat the local interaction. We are left with a non-interacting x-ray problem with a renormalized core-hole potential $Q' = Q - (n-1)U/2$, where $n > 1$ is

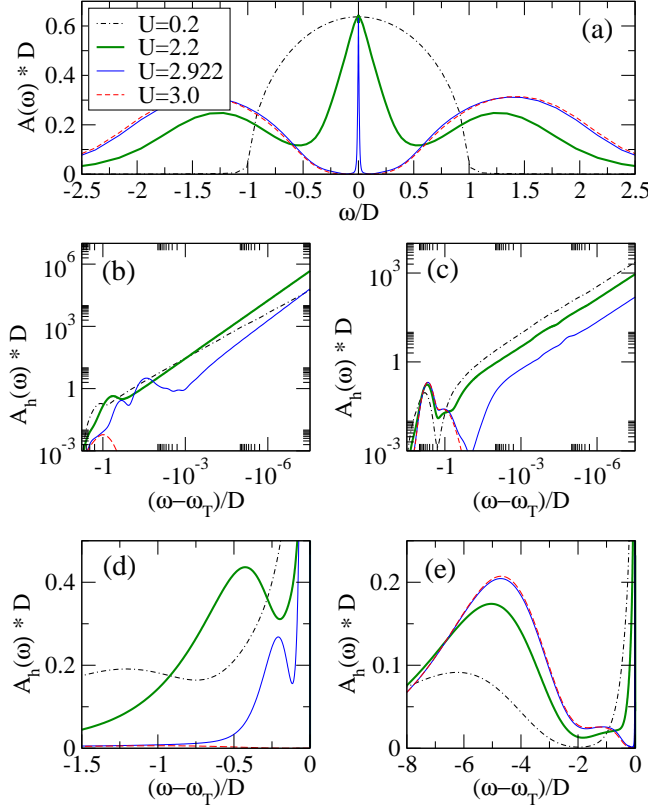


FIG. 2: (Color online) a) Valence spectra across the Mott transition in the electron-hole symmetric case. Note that for $U = 3.0$ the spectrum is gapped while for $U = 2.922$ there is a narrow peak at the Fermi level. b) Core-hole spectra for a core-hole potential $Q = 1.2$ across the MIT showing a power-law behavior close to the threshold in the metallic phase. c) Same as b) with $Q = 6.4$. d) and e) Detail of the high energy peaks of b) and c), respectively.

the charge on the impurity in the presence of the core-hole potential. In general we have $Q' < Q$ and we therefore expect the bound state peak (if present) to be shifted toward the threshold ($\omega - \omega_T \sim -Q'$) and the power-law to become more divergent as α is reduced to $\alpha_{HF} \sim 2/\pi^2 \arctan^2(2Q')$.

In Fig. 2b-e we show XPS spectra for different values of the interaction U and the core-hole potential Q . We obtain a power-law behavior (straight lines) throughout the metallic phase that disappears at the MIT. For small $U = 0.2$ the XPS spectrum can be understood within the Hartree-Fock scheme. This approximation, however, breaks down rapidly with increasing U as the system approaches the strongly correlated regime. We may argue in this regime that the width of the quasiparticle peak zD acts as an effective bandwidth for the x-ray problem.²³ While this allows us to understand the decrease of the onset energy for the power-law behavior (see Figs. 2b and 2c) it does not give the complete picture as we will see below.

Close to the MIT there are some important differences

in the spectra for the two values of Q shown in Fig. 2. While the power-laws in Fig. 2b for $Q = 1.2 < U_c/2$ have a significant increase in the slope when approaching the MIT (we have $\alpha \rightarrow 0$ for $U \rightarrow U_c$), those for $Q = 6.4$ in Fig. 2c have nearly parallel displacements with only a very small increase in the slope throughout the metallic phase. For $Q = 1.2$ the high energy peaks shift toward the edge with increasing U and disappear at the MIT leaving a delta-function peak at the threshold in the insulator. For $Q = 6.4 > U_c/2$ the main difference in the XPS spectra just below ($U = 2.922$) and above ($U = 3.0$) the MIT is the presence of the power-law in the metallic phase. The high energy peaks are essentially unchanged and the integrated intensity of the power-law vanishes at the MIT with $\alpha \neq 0$.

Some insight on the origin of these two distinct behaviors can be obtained by analyzing the atomic limit in the insulator. For values of Q such that $Q < U_c/2$, we have $Q < U/2$ throughout the insulating phase, which means that the core-hole potential is not strong enough (in the electron-hole symmetric case) to overcome the local repulsion and change the charge locally in the atomic level. The initial and final ground states will be identical and we therefore expect a peak at the threshold. In the opposite situation, $Q > U_c/2$, there will be a region close to the MIT in which the initial and final states have a different occupation of the atomic level. For these values of Q , the initial and final ground states are orthogonal and no peak is expected at the threshold.

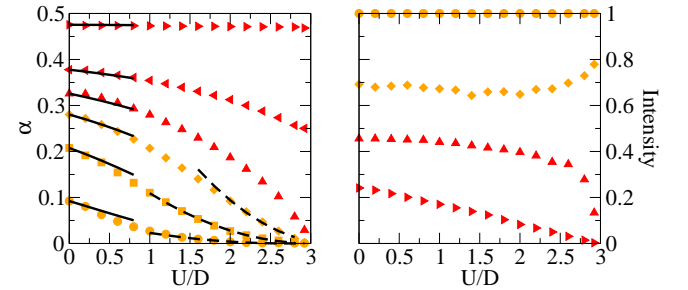


FIG. 3: (Color online) Left panel: Exponent α as a function of U , for different values of $Q = 12.8, 2.4, 1.6, 1.2, 0.8$, and 0.4 (from top to bottom). Results from NRG (symbols), Hartree-Fock results (solid lines), and parabolic fits $f(U) = AQ^2(U_c - U)^2$ with $A \sim 0.04$ (dashed lines). Right panel: integrated intensity of the power-law peak for $Q = 12.8, 1.6, 1.2$, and 0.4 (from bottom to top). The figure illustrates that the peak at threshold disappears at the MIT in two different manners, for $Q \gtrsim U_c/2$ and $Q \lesssim U_c/2$ (see text).

The results for the exponent and the integrated intensity of the power-law are summarized in Fig. 3. The exponent α increases with Q and decreases with increasing interaction. For small $U \ll Q, D$ the main effect of the interaction is a compensation (screening) of the core-hole potential that can be explained within a Hartree-Fock approach (solid lines in Fig. 3). For large $Q \gg U_c$, α is close to its maximum value $1/2$ and the interaction produces only a small reduction throughout the metal-

lic phase. The intensity of the peak at the threshold, however, vanishes continuously at the MIT. For small $Q < U_c/2$ the opposite behavior is observed with α vanishing at the transition while the integrated intensity of the peak remains finite.

The behavior of α can be understood through a Fermi liquid analysis. The Friedel sum rule gives an exact zero-temperature relation between the scattering phase-shift and the *total* charge ΔN (d -orbital plus conduction band) displaced when the core-hole potential is turned on,^{21,22} namely: $\delta = \pi\Delta N/2$. In the insulating phase, the valence band has a gap and the core-hole potential Q will not produce a displacement of charge ($\Delta N \equiv 0$) unless Q is large enough to overcome the local repulsion (i.e. $Q > U/2$). This reflects the incompressibility of the insulator. In contrast, in the metallic phase, charge will gather around the hole to screen it even for $Q \ll U$. The amount of displaced charge reflects the vanishing compressibility of the metal as the MIT is approached, so that we expect at small Q : $\Delta N \propto zQ$. Since Fermi-liquid analysis suggests that the Nozières and de Dominicis' value for the exponent [$\alpha = 2(\delta/\pi)^2$] is valid throughout the metallic phase even in the presence of interactions, this leads to a parabolic behavior $\alpha \propto 2(Qz/2)^2 \sim 0.05 Q^2(U_c - U)^2$, [where we used $z \sim 0.3(U_c - U)$]. This expression fits our data remarkably well, close to U_c and for $Q < U_c/2$ (see Fig. 3).

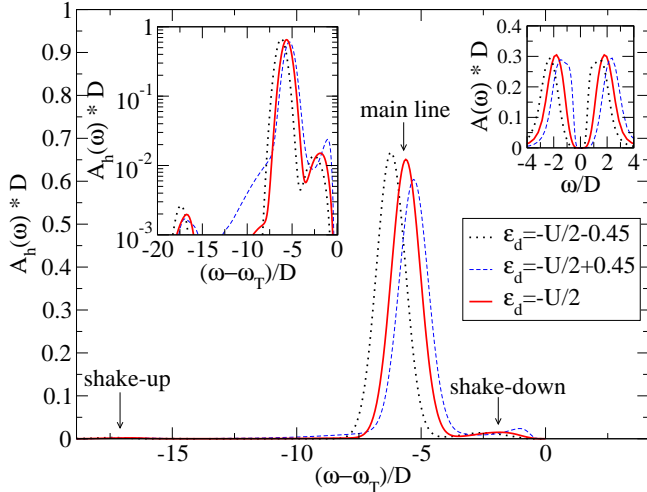


FIG. 4: (Color online) Core-hole photoemission spectra in the insulating phase ($U = 3.8$) for fixed $Q = 2U$ and three values of ϵ_d . Left inset: in a logarithmic scale three peaks can be identified. Right inset: Hubbard bands in the valence spectra.

IV. MOLECULAR ORBITAL APPROXIMATION

The intensity and position of the peaks in the insulating phase can be understood in the molecular orbital approximation. The effective bath in DMFT is modeled with a single site having a Hubbard interaction U and

energy ϵ_d . The resulting two site Hubbard model can be solved analytically. In the absence of the core-hole potential, the ground state is in a subspace with 2 electrons. When the core-hole potential is small ($Q \lesssim U/2$) the ground state is in the same charge sector and is essentially unchanged. Therefore, the XPS spectrum has a delta-function peak at the threshold which carries almost all the spectral weight (see Fig. 5). For large $Q \gtrsim U/2$ the final ground state is in a subspace with three electrons and is therefore orthogonal to the initial ground state ($\langle 0_f | 0_i \rangle = 0$). In this regime three peaks can be identified in the XPS spectra and there is no peak at the threshold. The main peak has a weight $1 - \frac{3}{Q^2} - \frac{1}{U^2} + \dots$ and there are two satellites at a distance $\sim U + Q$ (shake-up) and $\sim Q - U$ (shake-down). The shake-down peak is at a distance ϵ_d from the threshold and has a larger intensity $(\frac{1}{2U^2} + \frac{1}{UQ} + \frac{3}{2Q^2} + \dots)$ than the shake-up peak $(\frac{1}{2U^2} - \frac{1}{UQ} + \frac{3}{2Q^2} + \dots)$.

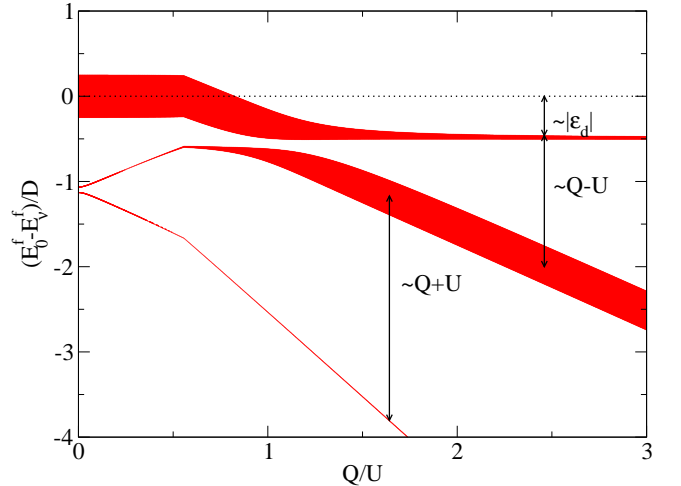


FIG. 5: (Color online) Molecular orbital results for the position of the XPS peaks in the insulating phase. The thickness of the lines is proportional to the peak intensity. Parameters are $U = 3.8D$, $\epsilon_d = -U/2$, and $\epsilon_h = 0$.

The molecular results are in excellent agreement with the numerical results in the insulating phase (see Fig. 4). The shake-up (-down) peak is associated to the creation of an electron (hole) in the upper (lower) Hubbard band and has an intrinsic width of order D . For a finite hole lifetime (finite temperature) the spectrum will have an additional Lorentzian (Gaussian) broadening²⁴. We note that, although it is likely to be difficult in practice, a measurement of the *three* peaks provides in principle a direct estimate of U . We stress that a measurement of the shake-down peak alone is not enough for such an estimation. As shown in Fig. 4, a change in ϵ_d only produces a small redistribution of the spectral intensity and a global shift of the peaks relative to the threshold. The molecular orbital results also give a good estimation for the position of the peaks away from the threshold in the metallic phase (see Fig. 2e).

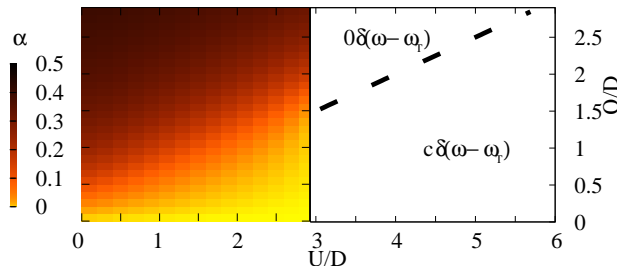


FIG. 6: (Color online) Behavior of the XPS spectra at the edge as a function of U and Q . Left panel: coefficient α of the power-law divergence in the metal. Right panel: below the line $Q \sim U/2$ the spectra present a delta-function peak in the insulator.

V. SUMMARY AND CONCLUSIONS

In summary, we have studied theoretically the behavior of the core-level photoemission spectra across the correlation-driven MIT. Away from the photoemission threshold and far from the MIT, both the position and relative intensity of the peaks are well described by a molecular orbital approach. Close to the threshold or to the MIT, more sophisticated techniques (such as DMFT and NRG) are necessary to describe the spectra. The changes in the XPS spectra across the MIT may be used to detect the transition. A symmetric peak (or no peak) at the edge implies an insulating phase, while an asymmetric peak or a power-law corresponds to a metal. For

large $Q > U/2$ there are three peaks in the XPS spectra. While the shake-up peak is usually weak and will probably be difficult to detect, its observation in conjunction with the shake-down peak allows in principle for a direct estimation of U .

The most interesting results concern the behavior of the XPS spectra at the threshold as summarized in Fig. 6. In the metallic phase there is a power-law behavior with an exponent $\alpha - 1$, where α depends on both the local interactions on the band U and the intensity of the core-hole potential Q . The power-law regime is restricted to an energy range $\sim zD$ close to the threshold and disappears at the MIT. For $Q \lesssim U_c/2$ the exponent α depends strongly on U and vanishes as $\sim z^2$ at the transition. The integrated intensity, however, remains finite giving rise to a delta-function peak in the insulator. In contrast, for $Q \gtrsim U_c/2$, α is finite at the transition but the integrated intensity of the peak vanishes and there is no delta-function peak in the insulator. Future high-resolution experiments might be able to test our theoretical predictions for the edge-singularity in a correlated metal close to the MIT.

Acknowledgments

We are thankful to M. Altarelli, G. Kotliar, G. Panaccione, A. Poteryaev, and G. Sawatzky for useful discussions.

-
- ¹ P. W. Anderson, Phys. Rev. Lett. **18**, 1049 (1967).
² G. D. Mahan, Phys. Rev. **163**, 612 (1967).
³ P. Nozières and C. T. De Dominicis, Phys. Rev. **178**, 1097 (1969).
⁴ S. Doniach and M. Sunjić, J. Phys. C **3**, 285 (1970).
⁵ D. K. K. Lee and Y. Chen, Phys. Rev. Lett. **69**, 1399 (1992).
⁶ V. Meden, P. Schmitteckert, and N. Shannon, Phys. Rev. B **57**, 8878 (1998).
⁷ K. Horiba, M. Taguchi, A. Chainani, Y. Takata, E. Ikenaga, D. Miwa, Y. Nishino, K. Tamasaku, M. Awaji, A. Takeuchi, et al., Phys. Rev. Lett. **93**, 236401 (2004).
⁸ H.-D. Kim, H.-J. Noh, K. H. Kim, and S.-J. Oh, Phys. Rev. Lett. **93**, 126404 (2004).
⁹ M. Taguchi, A. Chainani, N. Kamakura, K. Horiba, Y. Takata, M. Yabashi, K. Tamasaku, Y. Nishino, D. Miwa, T. Ishikawa, et al., Phys. Rev. B **71**, 155102 (2005).
¹⁰ G. Panaccione, M. Altarelli, A. Fondacaro, A. Georges, S. Huotari, P. Lacovig, A. Lichtenstein, P. Metcalf, G. Monaco, F. Offi, et al., Phys. Rev. Lett. **97**, 116401 (2006).
¹¹ A. Georges, G. Kotliar, W. Krauth, and M. J. Rozenberg, Rev. Mod. Phys. **68**, 13 (1996).
¹² K. Ohtaka and Y. Tanabe, Rev. Mod. Phys. **62**, 929 (1990).
¹³ V. L. Libero and L. N. Oliveira, Phys. Rev. B **42**, 3167 (1990).
¹⁴ K. G. Wilson, Rev. Mod. Phys. **47**, 773 (1975).
¹⁵ W. Hofstetter, Phys. Rev. Lett. **85**, 1508 (2000).
¹⁶ R. Bulla, T. A. Costi, and D. Vollhardt, Phys. Rev. B **64**, 045103 (2001).
¹⁷ F. B. Anders and A. Schiller, Phys. Rev. Lett. **95**, 196801 (2005).
¹⁸ T. A. Costi, A. C. Hewson, and V. Zlatić, J. Phys.: Condens. Matter **6**, 2519 (1994).
¹⁹ R. Bulla, Phys. Rev. Lett. **83**, 136 (1999).
²⁰ T. A. Costi, J. Kroha, and P. Wölfle, Phys. Rev. B **53**, 1850 (1996).
²¹ J. Friedel, Phil. Mag. **43**, 153 (1952).
²² D. C. Langreth, Phys. Rev. **150**, 516 (1966).
²³ A related phenomenon was discussed in Ref. [20].
²⁴ The numerical procedure employed gives an additional width to the high energy peaks [16].